



Recent Correlation & Fluctuation highlights from the STAR Experiment

Rutik Manikandhan (University of Houston)
for the STAR Collaboration



Supported in part by
U.S. DEPARTMENT OF
ENERGY

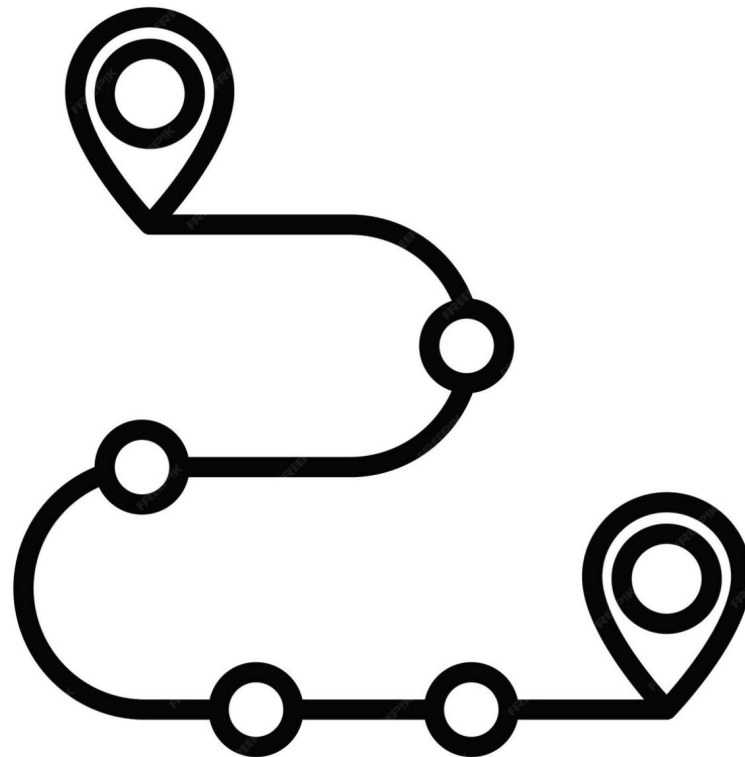
New Frontiers in Physics
ICNFP 2025

<https://indico.cern.ch/e/icnfp2025>

Outline

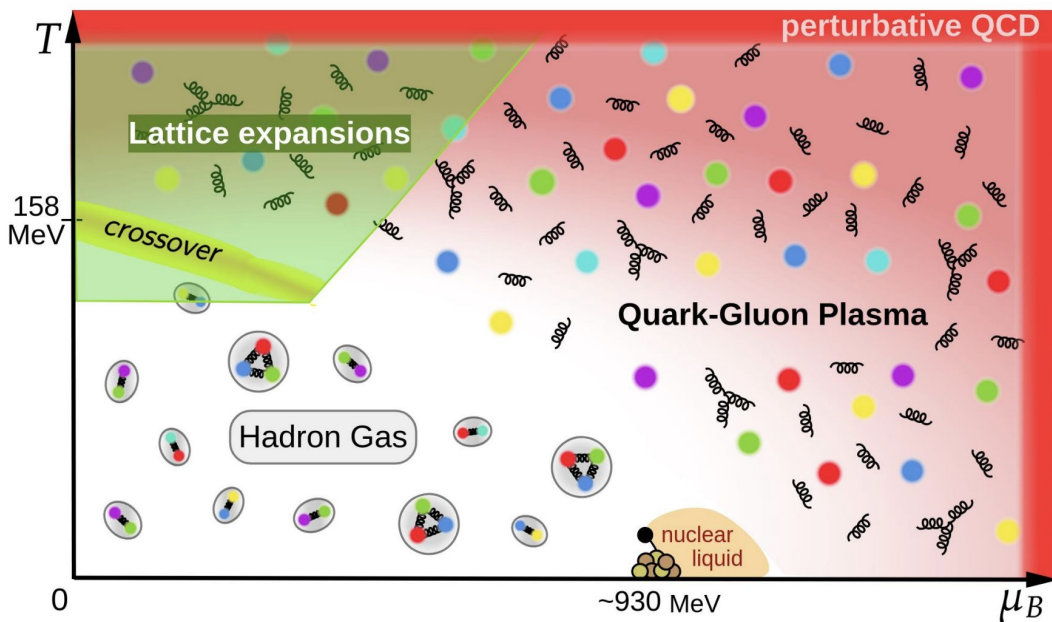


- ❖ Introduction
- ❖ STAR Experiment
- ❖ Results:
 - Critical Point Searches
 - Femtoscopy
 - Exotic Nuclei
- ❖ Summary

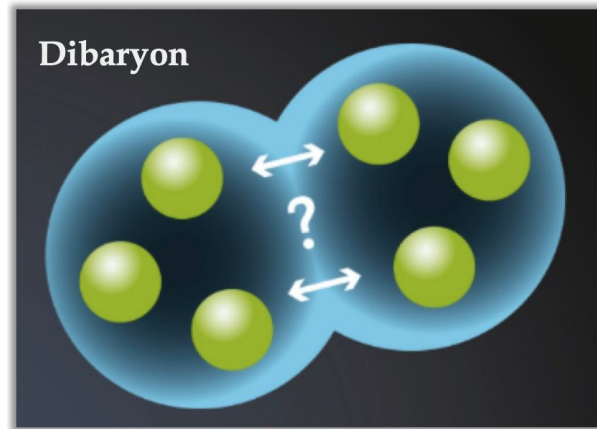


Probing QCD structure through correlations

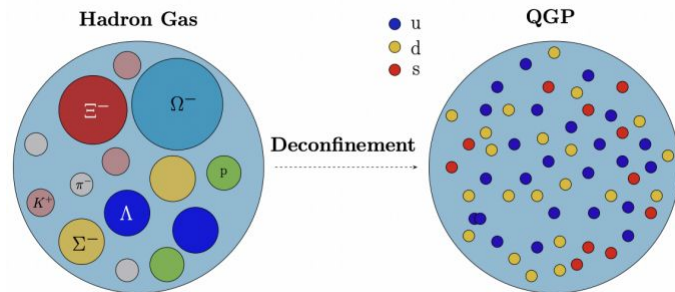
QCD Phase Diagram



Exotic Nuclei



Phase Transition

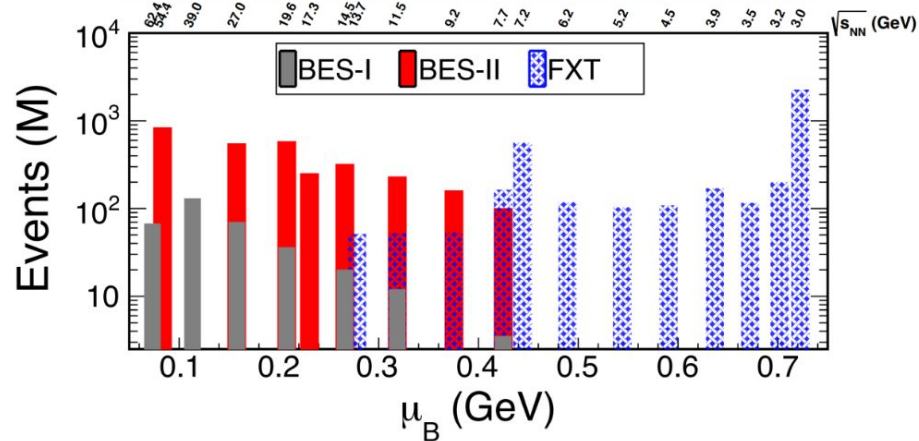
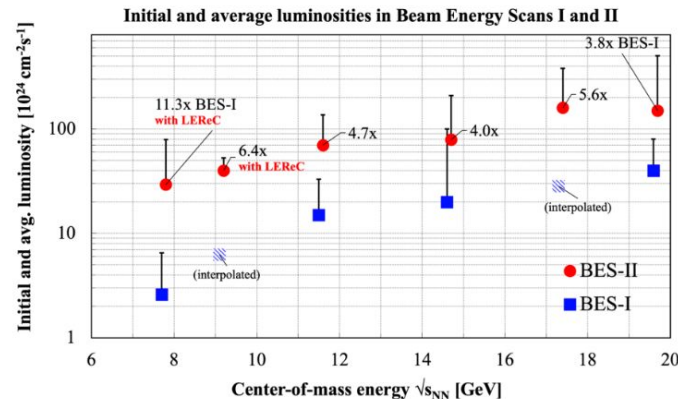
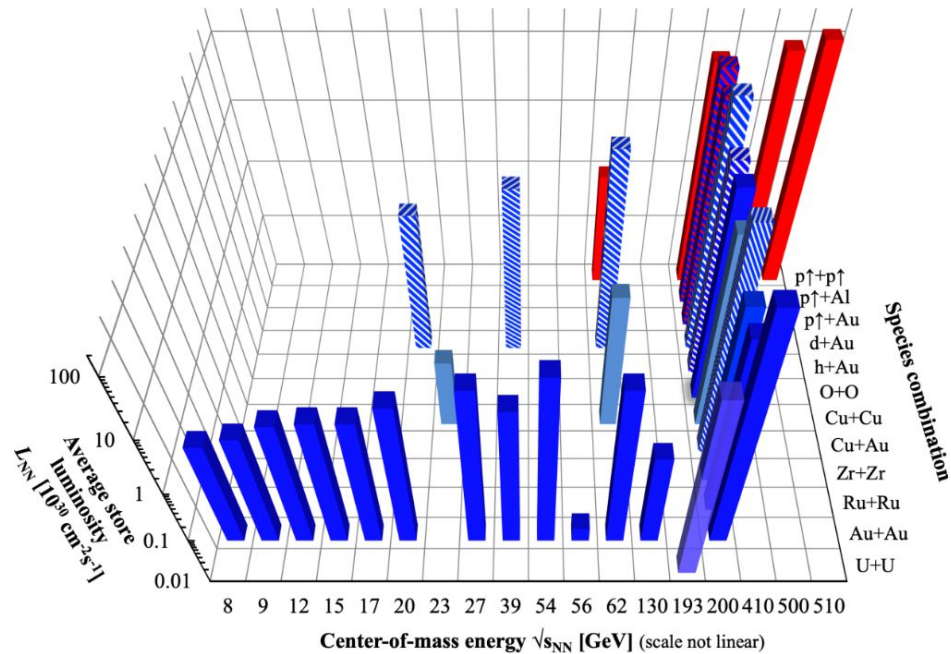


STAR Experiment

Extremely Versatile!



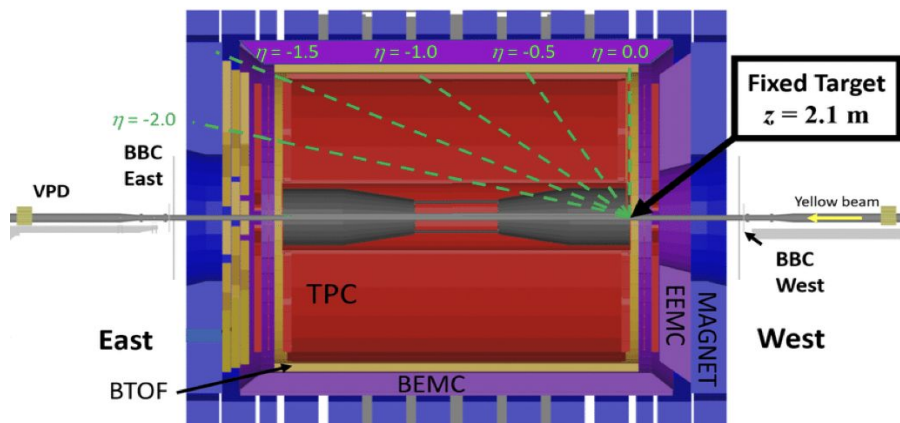
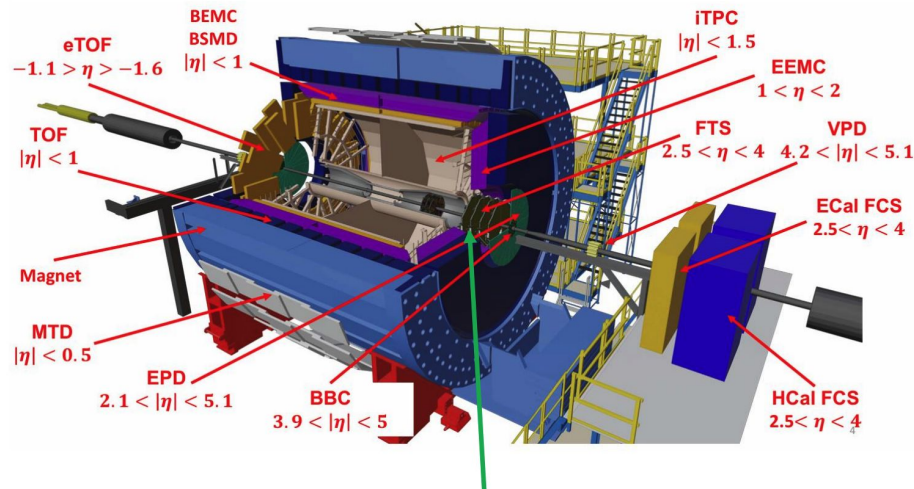
RHIC energies, species combinations and luminosities (Run-1 to 22)



STAR Detector



- ❖ Multiple sub detector systems
- ❖ Excellent particle identification capabilities
- ❖ Full azimuthal acceptance



Target (Fixed Target mode)

- ❖ Gold Target fixed at west end of the detector
- ❖ TPC Acceptance :
➤ $\eta : [-2,0]$ (lab frame)
- ❖ PID Acceptance (TPC + ToF):
➤ $\eta : [-1.5,0]$ (lab frame)

Critical Point searches

Femtoscscopy

Exotic Nuclei

Proton Multiplicity Cumulants



Cumulants:

n = net-proton multiplicity
in an event

$$\delta n = n - \langle n \rangle$$

$$C_1 = \langle n \rangle$$

$$C_2 = \langle \delta n^2 \rangle$$

$$C_3 = \langle \delta n^3 \rangle$$

$$C_4 = \langle \delta n^4 \rangle - 3 \langle \delta n^2 \rangle^2$$

Factorial Cumulants:

$$\kappa_1 = C_1$$

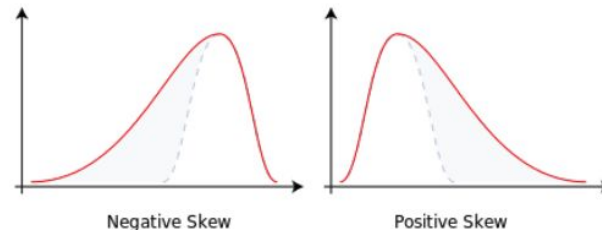
$$\kappa_2 = -C_1 + C_2$$

$$\kappa_3 = 2C_1 - 3C_2 + C_3$$

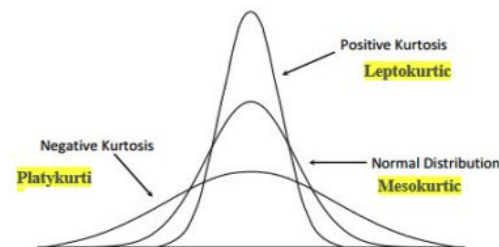
$$\kappa_4 = -6C_1 + 11C_2 - 6C_3 + C_4$$

Cumulants quantify characteristics
of distributions:

Skewness: C_3/C_2



Kurtosis: C_4/C_2



Cumulants for CP Search



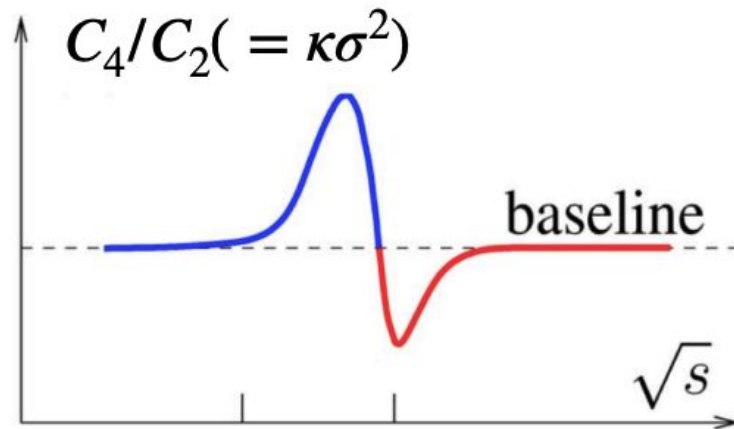
Cumulants are related to the correlation length

$$C_2 \sim \zeta^2$$

$$C_4 \sim \zeta^7$$

Cumulants ratios are related to ratios of susceptibilities

$$\frac{C_{4q}}{C_{2q}} = \frac{\chi_4^q}{\chi_2^q}$$



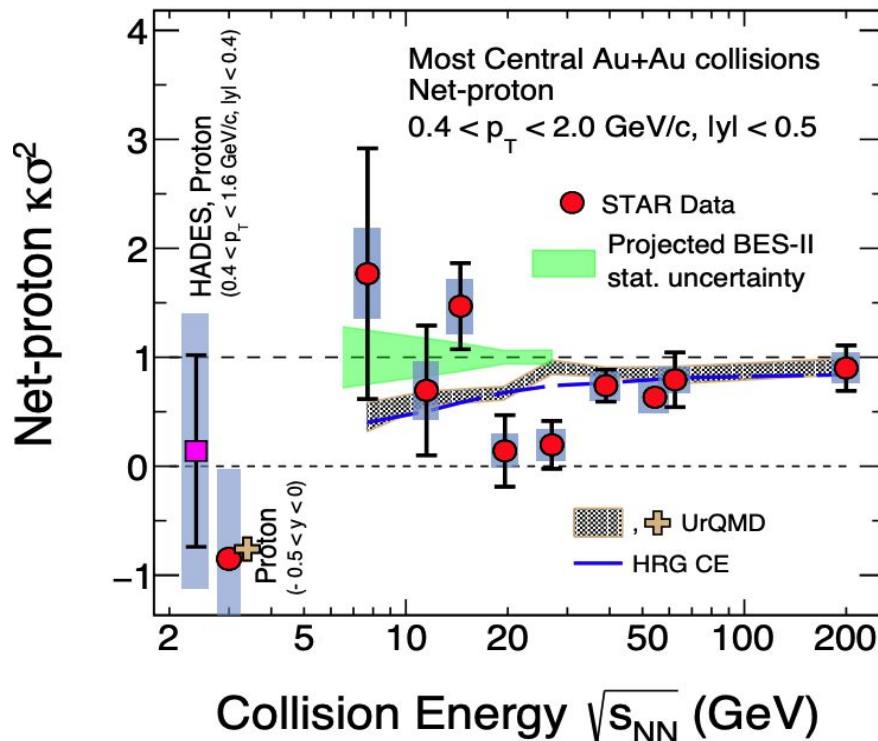
Non-monotonic dependence on collision energy (\sqrt{s}) predicted to be a signature of critical behaviour

M. A. Stephanov, PRL 107 (2011) 052301

BES-I Measurement of Kurtosis



- ❖ Observed hint of non-monotonous trend in BES-I (3σ)
- ❖ Robust conclusion requires confirmation from precision measurement from BES-II.
- ❖ Extend reach to even lower collision energies with FXT program energies



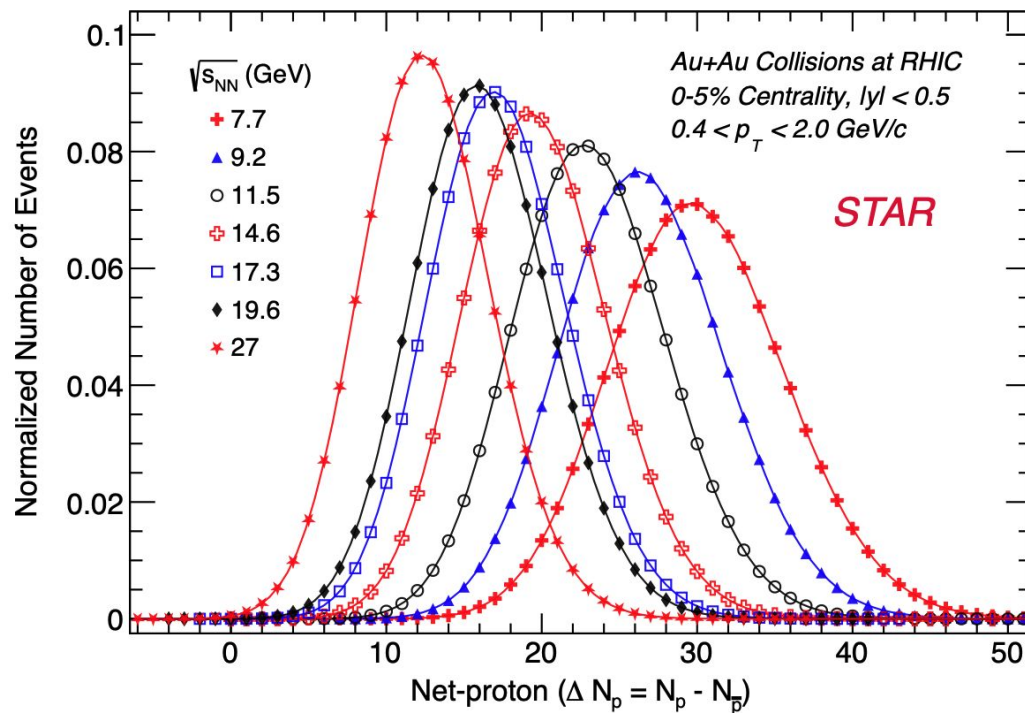
STAR : PRL 127, 262301 (2021), PRC 104, 24902 (2021), PRL 128, 202302 (2022),
PRC 107, 24908 (2023)
HADES: PRC 102, 024914 (2020)

BES-II Scan of Proton Cumulants



Net-proton Distributions:

- Raw net-proton distributions from BES-II (Collider): Uncorrected for detector efficiency.
- Mean increases with decreasing collision energy (baryon stopping).
- Larger width leads to larger Stat. uncertainties.



arXiv:2504.00817

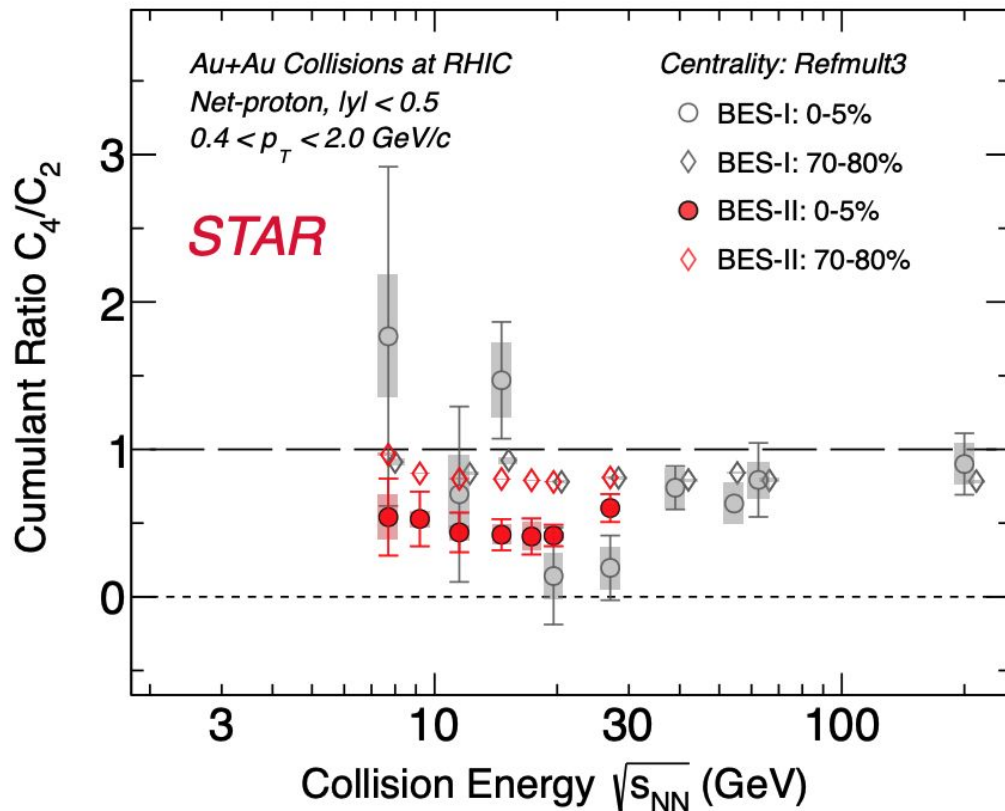
BES-II Vs BES-I



- ❖ Two different centrality classes shown
- ❖ Results consistent between BES-I and BES-II:

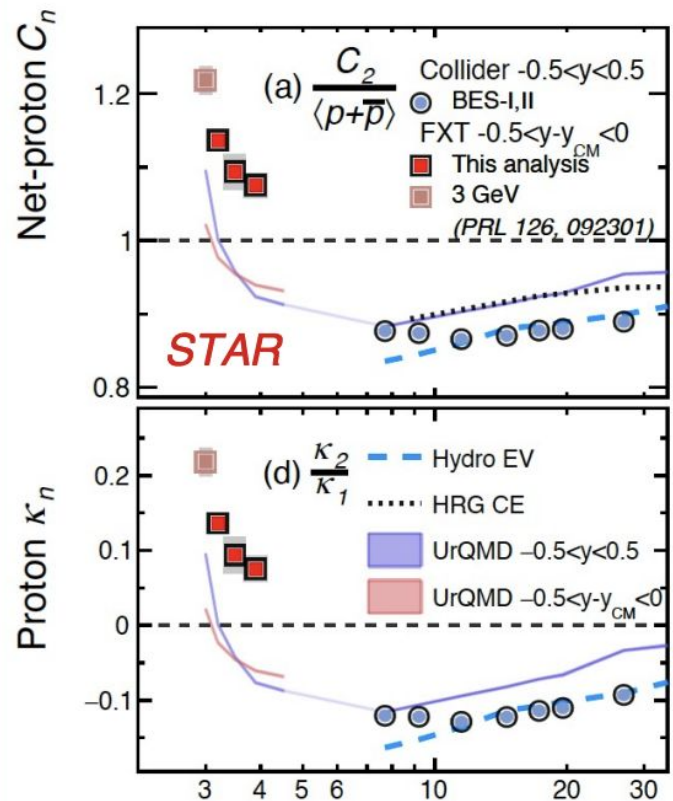
$\sqrt{s_{NN}}$ (GeV)	0-5%	70-80%
7.7	1.0σ	0.9σ
11.5	0.4σ	1.3σ
14.6	2.2σ	2.5σ
19.6	0.7σ	0.0σ
27	1.4σ	0.2σ

- ❖ In BES-II we go lower in energy



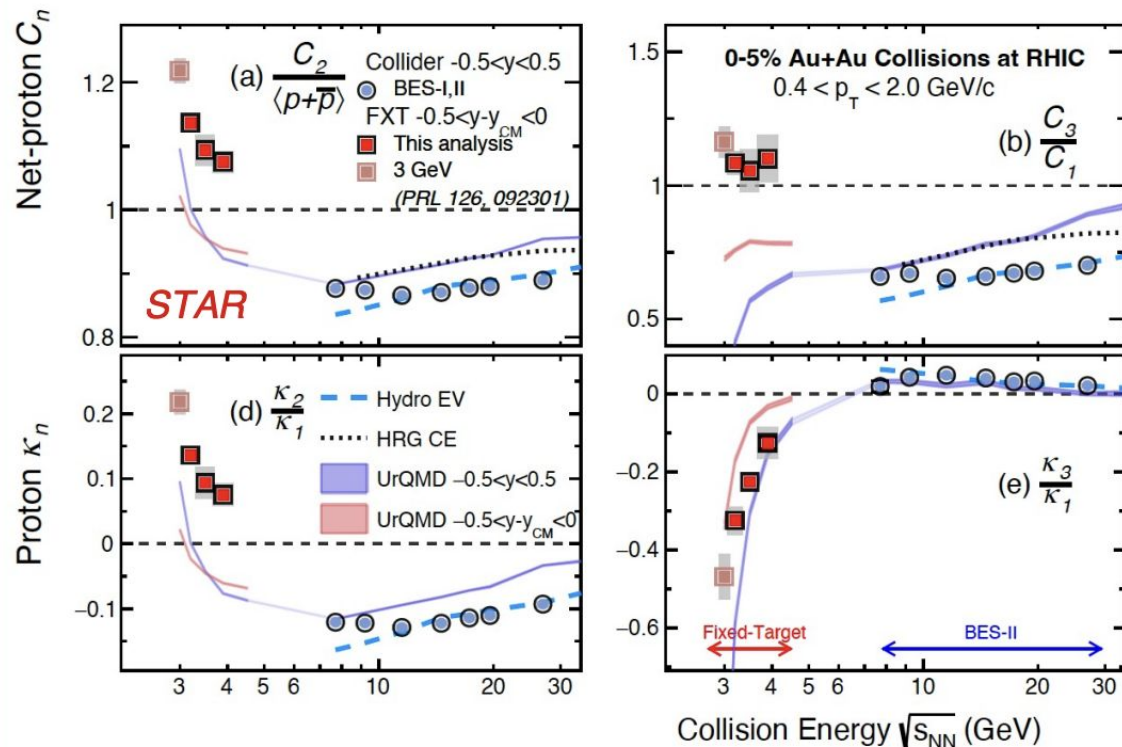
arXiv:2504.00817

Proton Cumulants vs Collision Energy



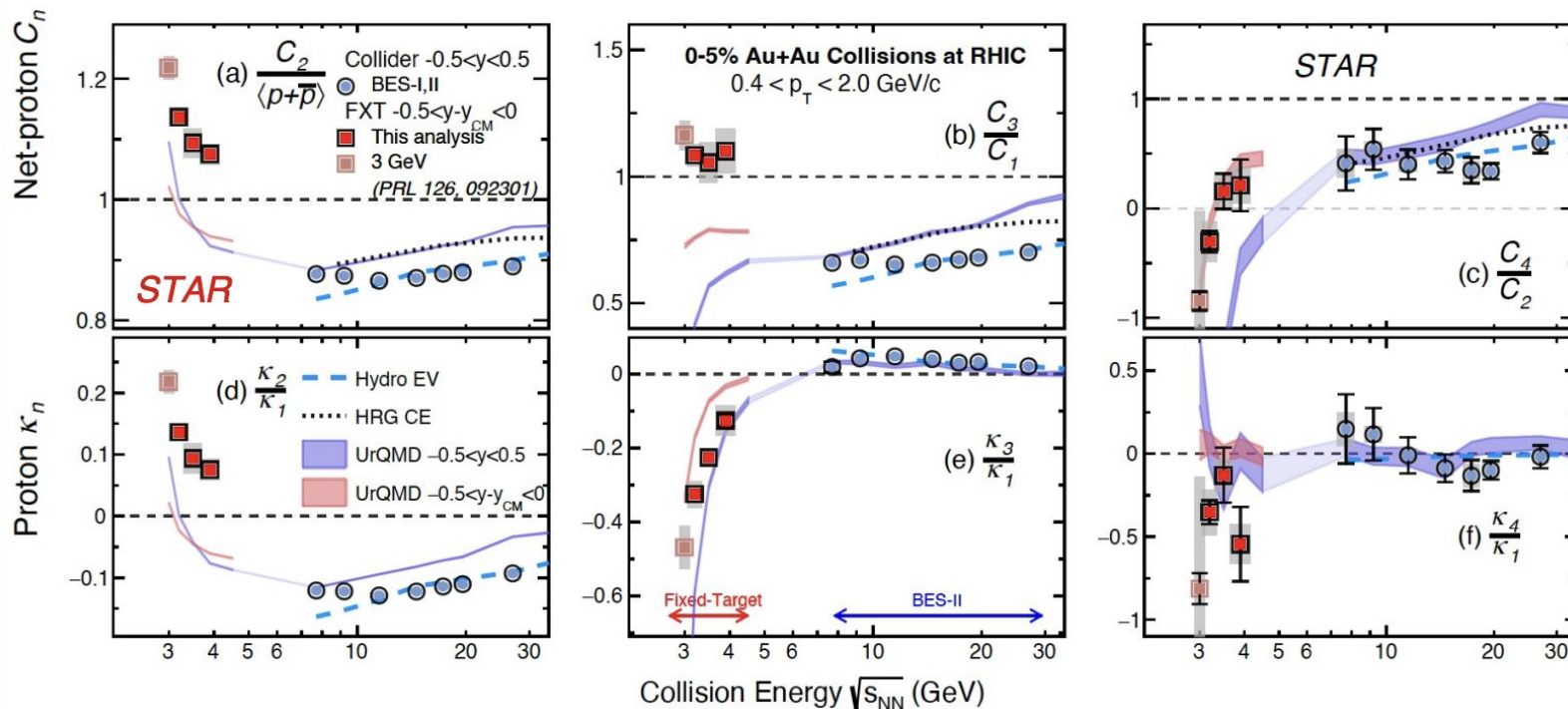
- ❖ Collider C_2/C_1 and κ_2/κ_1 show monotonous increase as predicted by Hydro
- ❖ Fixed-target C_2/C_1 and κ_2/κ_1 monotonically decrease, as predicted by UrQMD
- ❖ Significant enhancement of cumulants above baseline at fixed target energies.

Proton Cumulants vs Collision Energy



- ◆ C_3/C_1 shows no strong energy dependence, similar to UrQMD
- ◆ κ_3/κ_1 monotonically increases, as predicted
- ◆ Significant deviations from non-critical baseline at C_3/C_1 and κ_3/κ_1 at fixed target energies

Proton Cumulants vs Collision Energy



❖ C_4/C_2 right on baseline for fixed target, maximum deviation seen at 19.6 GeV for significance of deviation $\sim 2 - 5\sigma$

❖ κ_4/κ_1 shows no strong energy dependence within uncertainties

Transverse Momentum Correlations



- ❖ High-energy kinematics and Quantum Chromodynamics (QCD) **generate correlations** between the first partons produced at the onset of a nuclear collision [1].
- ❖ Transverse momentum correlators have been proposed as a **measure of these correlations** and as a probe for the critical point of quantum chromodynamics [2].

$$C_m = \langle \Delta p_{t,i}, \Delta p_{t,j} \rangle$$

$$\langle (p_{t,i} - \langle p_t \rangle)(p_{t,j} - \langle p_t \rangle) \rangle$$

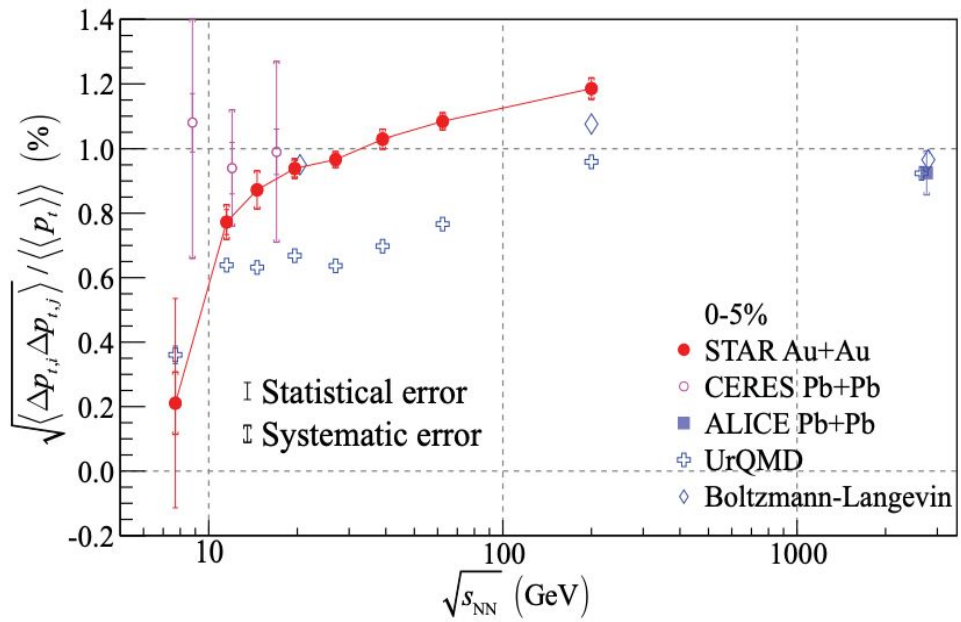
$$i \neq j$$

[1]: S. Gavin. Physical Review Letters, 92(16)

[2]: ALICE, Phys. Part. Nuclei 51,2020

Correlator Vs Collision energy

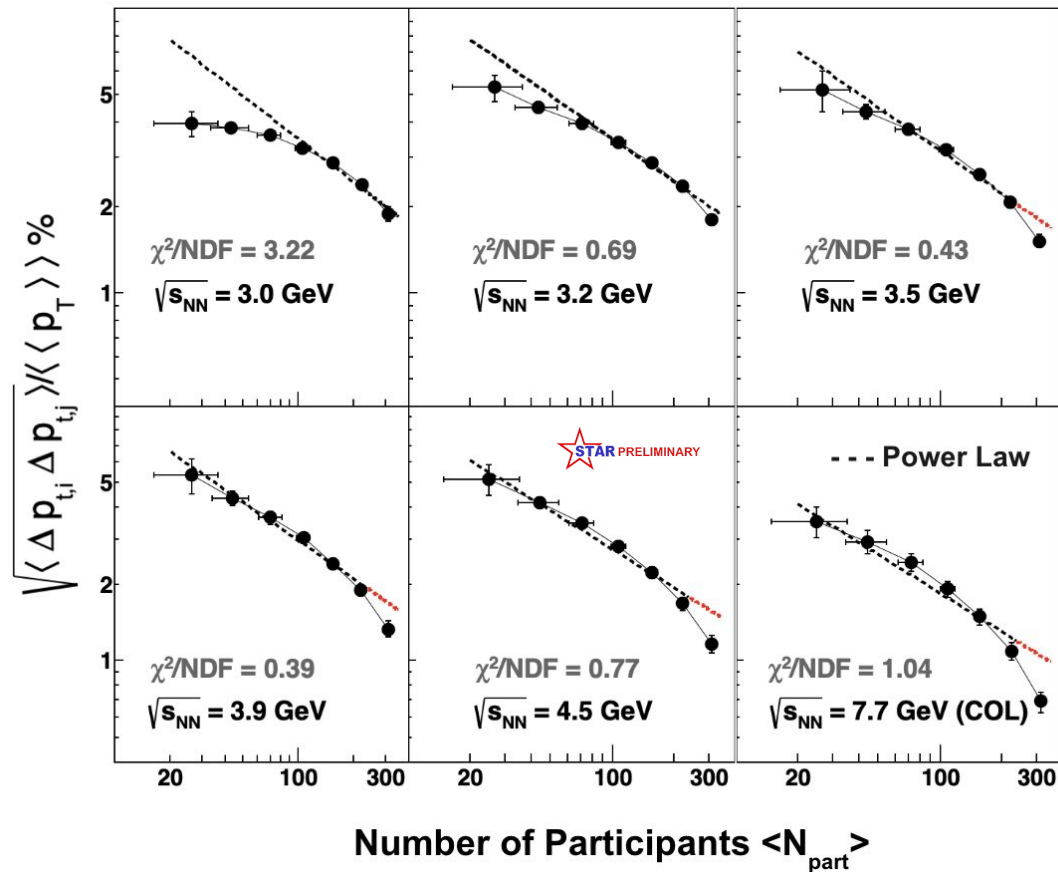
- ❖ The correlation observable may have a trivial dependence on energy, so we **scale it with $\langle\langle p_T \rangle\rangle$** .
- ❖ **Efficiency independent** observable.
- ❖ Make a direct comparison with the CERES and ALICE.
- ❖ Monotonous dependence on collision energy observed.



STAR, Phys.Rev.C72:044902,2005
 ALICE, Eur. Phys. J. C 74, 2014
 CERES, Nucl.Phys.A811:179-196,2008

Correlator Vs Centrality

- ❖ The black dashed lines represent a power law fit given by $:A(\sqrt{s_{NN}})*1/(N_{part})^{0.5}$, upto $N_{part} \sim 240$
- ❖ Red dashed line is an extrapolation to show deviation from Independent Sources behaviour
- ❖ Deviations from this scaling behavior may signal the onset of collective effects, such as a phase transition, or critical phenomena that depend on particle density



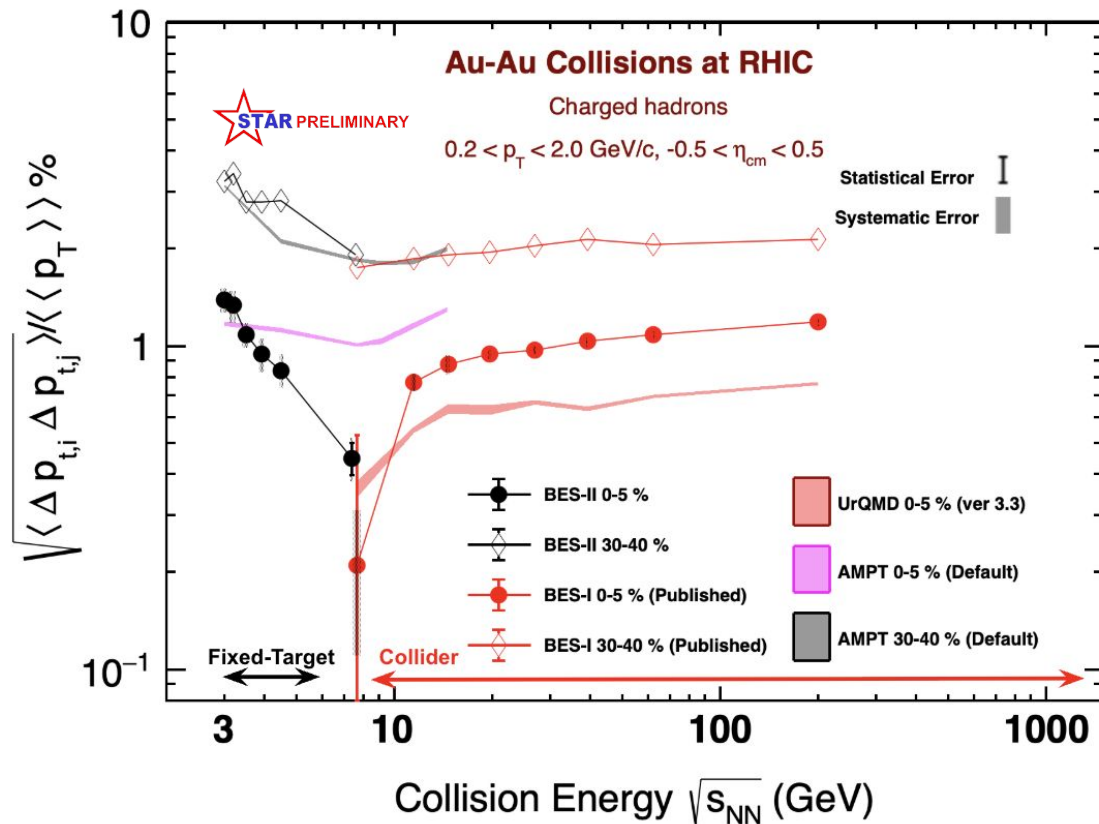
S. Bhatta et. al. Phys. Rev. C 105, 024904

M. Cody et. al. Phys. Rev. C 107, 014909

Correlator Vs Collision energy



- ❖ Two-particle correlator displays significant non-monotonic behavior as a function of collision energy in the 0–5% centrality bin.
- ❖ We make comparisons to different versions of UrQMD and AMPT transport code and observe deviations from both the models.

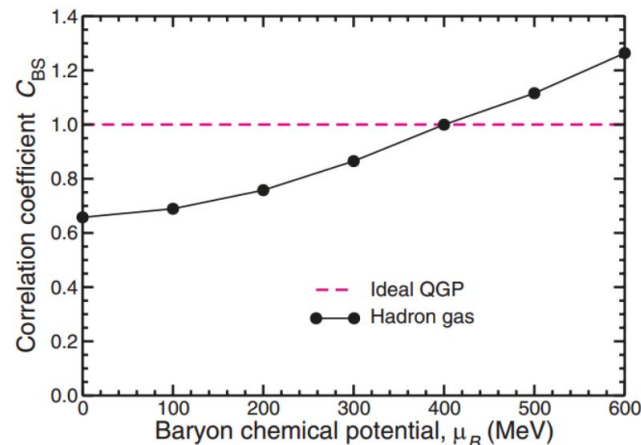
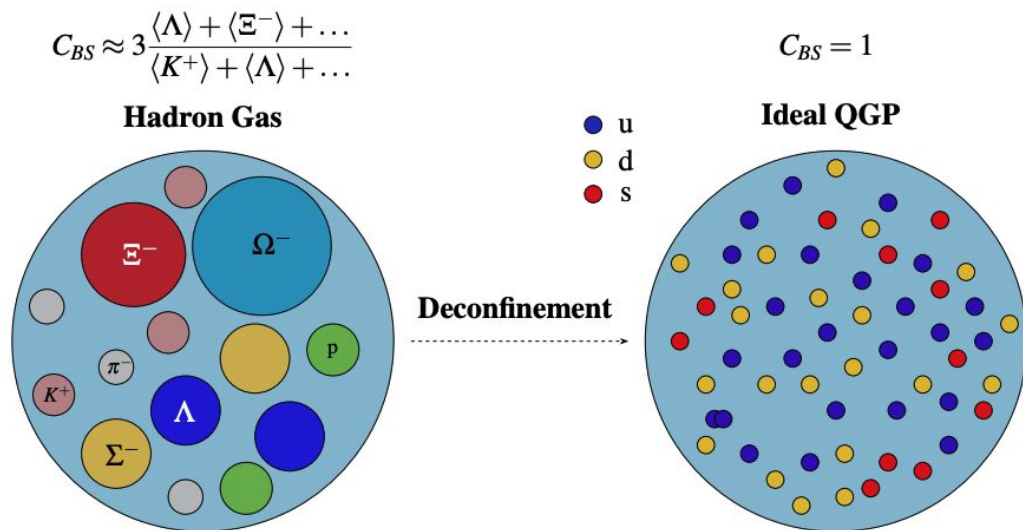


Baryon-Strangeness Correlations

Baryon-Strangeness Correlations (C_{BS}) is proposed to diagnose the change of phases in the matter created in the heavy-ion collisions, which is expressed as:

$$C_{BS} = -3 \frac{\langle BS \rangle_c}{\langle S^2 \rangle_c} = -3 \frac{\langle BS \rangle - \langle B \rangle \langle S \rangle}{\langle S^2 \rangle - \langle S \rangle^2}$$

V. Koch, A. Majumder and J. Randrup, Phys. Rev. Lett. 95, 182301 (2005)



Baryon-Strangeness Correlations

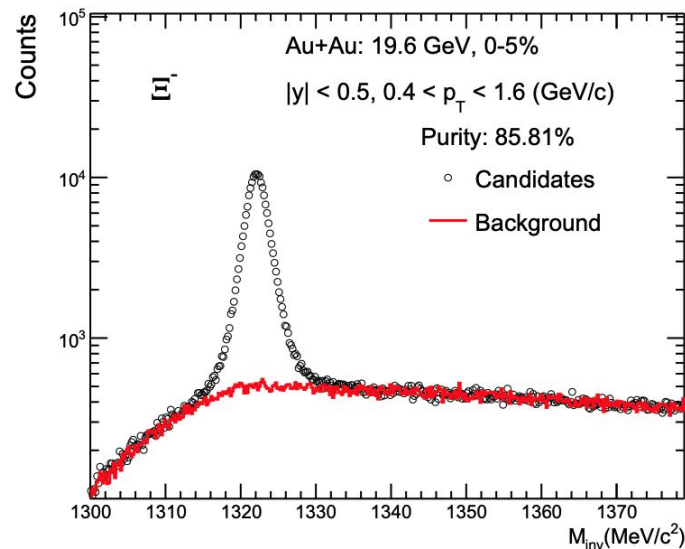
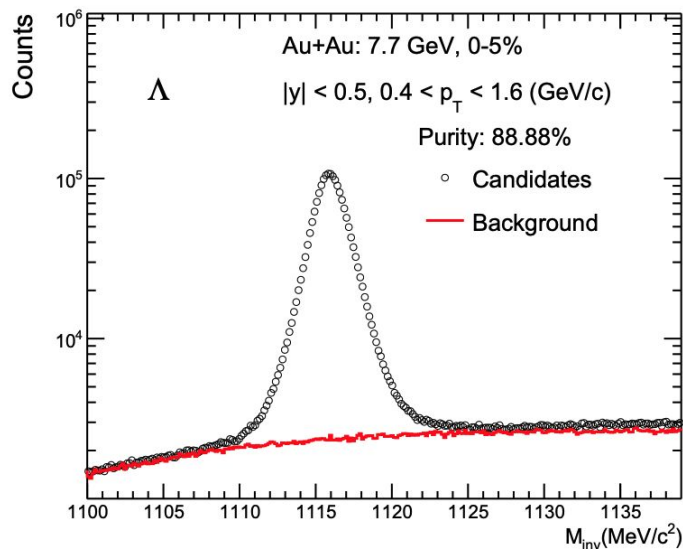


Experimentally, the baryon number (B) and strangeness (S) are defined as :

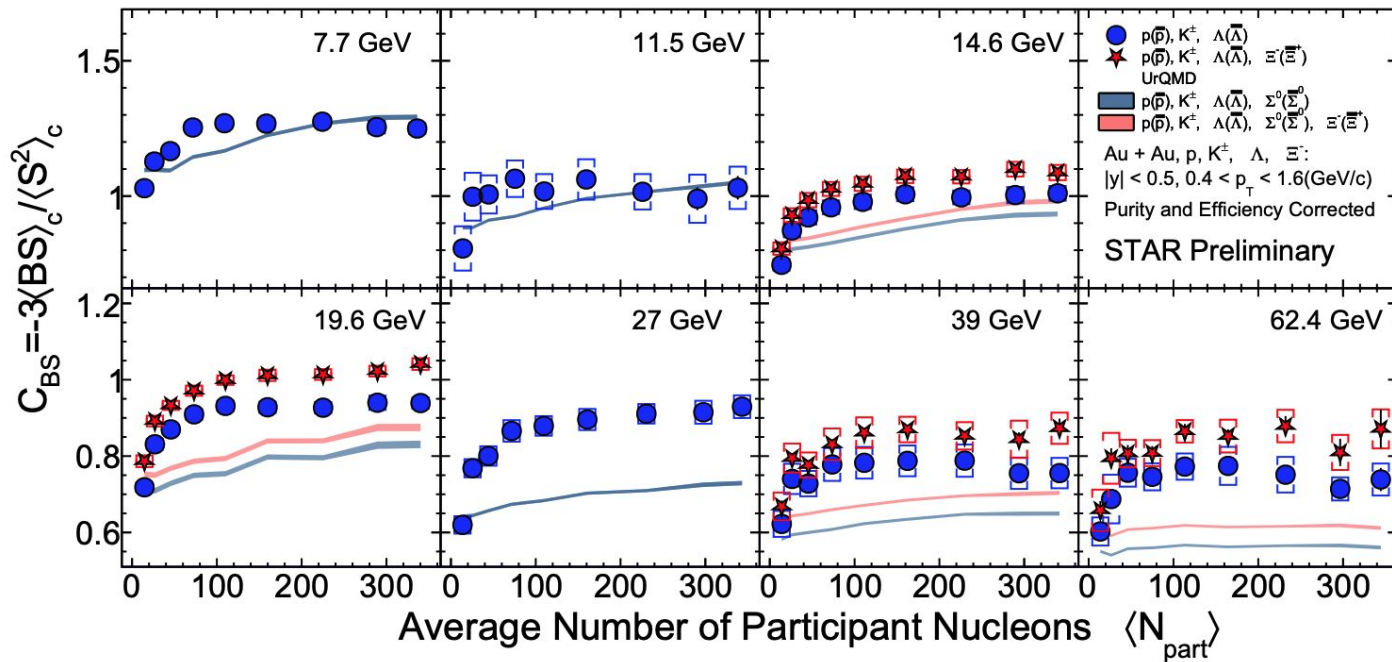
$$\text{net-B} = \delta p + \delta \Lambda (+ \delta \Xi^-)$$

$$\text{net-S} = \delta K^+ - \delta \Lambda (-2 \delta \Xi^-)$$

Where $\delta A = A - \text{anti } A$



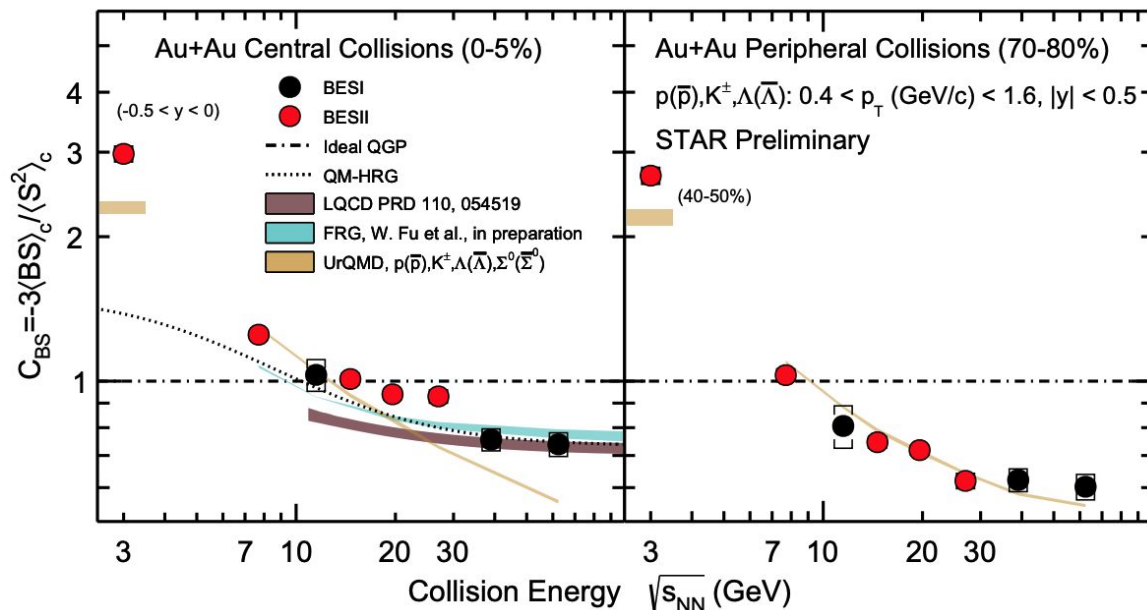
C_{BS} Vs Centrality



- ❖ C_{BS} gradually increases with centrality and saturates in the mid-central collision.
- ❖ UrQMD describes low energy data better than high energy data.

C_{BS} Vs Collision energy

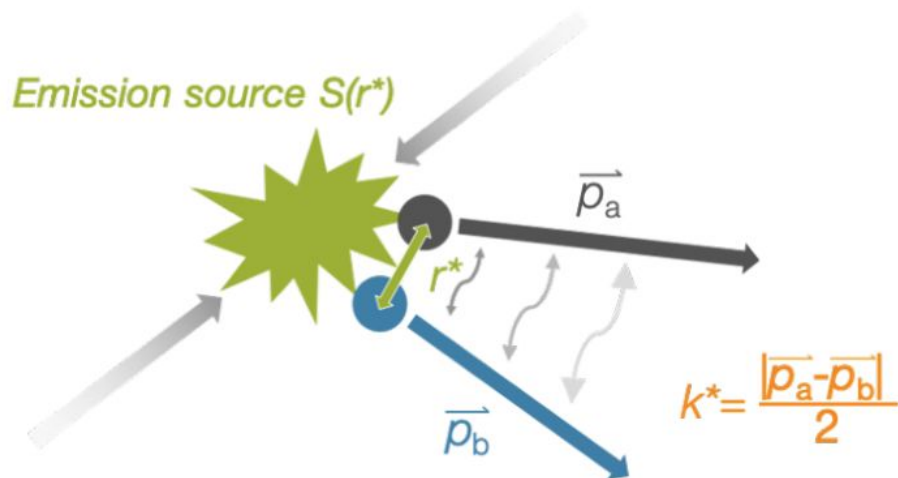
- ❖ 39 and 62.4 GeV are consistent with partonic calculations, namely functional renormalization group (FRG) and LQCD calculations
- ❖ The results of 7.7 and 11.5 GeV are better described by hadronic transport model UrQMD
- ❖ 14.6, 19.6 and 27 GeV cannot be reproduced by either of the calculations
- ❖ Large value observed of CBS at 3 GeV is consistent with baryon rich environment.
- ❖ For peripheral collisions, the energy dependence from 7.7 to 62.4 GeV can be described by UrQMD.



Critical Point searches

Femtoscscopy

Exotic Nuclei



HBT technique adopted in high-energy physics, where, like sign particle correlation are used to determine the radius and lifetime of the hadronic matter produced during heavy-ion collisions

Obtain spatial and temporal information on particle-emitting source at kinetic freeze-out to study collision dynamics dependence on EoS.

$$C(k^*) = \underbrace{\int \boxed{S(r^*)} \left| \Psi(k^*, r^*) \right|^2 d^3 r^*}_{\text{Model}} = \underbrace{\frac{A(k^*)}{B(k^*)}}_{\text{Measurement}}$$

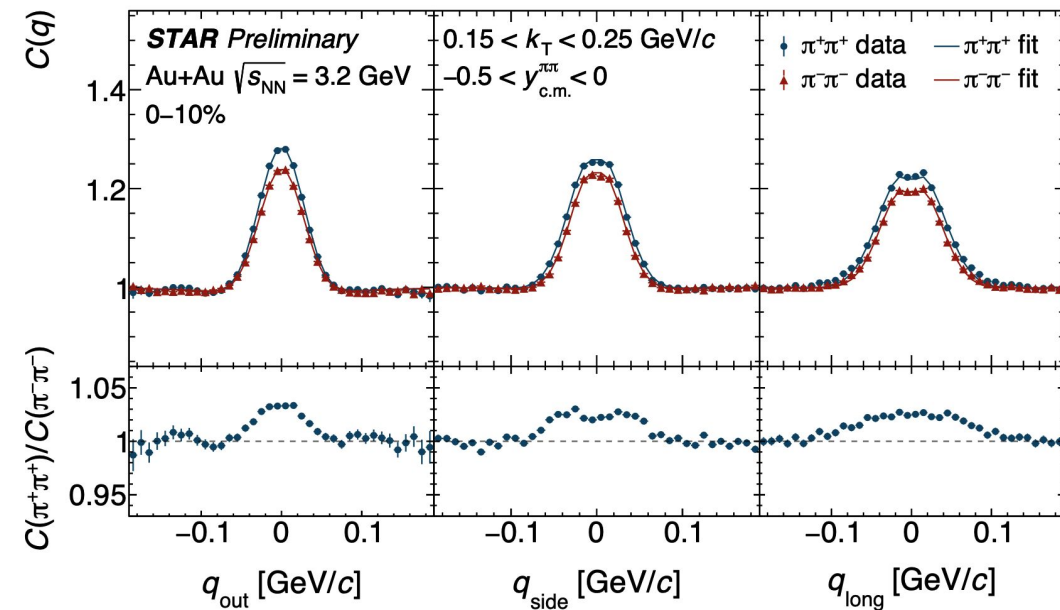


[illegible]

- ❖ **Experimental measurement** : $C(\vec{q}) = A(\vec{q})/B(\vec{q})$
 - **Relative momentum** : $\vec{q} = \vec{p}_1 - \vec{p}_2$
 - $A(\vec{q})$: **measured distribution of q within the same event containing quantum statistic (QS) correlation and final state interactions.**
 - $B(\vec{q})$: **background distribution of q of two tracks from different events, where physical correlations are absent.**
- ❖ **These vectors are projected onto a frame of reference, co-moving longitudinally (LCMS):**
 - q_{out} : **along pair transverse momentum (k_T)**
 - q_{long} : **along beam direction**
 - q_{side} : **perpendicular to the other two axes.**

G. Bertsch, M. Gong, M. Tohyama, PRC 37, 1896 (1988)

Charged pion correlation function



- ◆ About 3% difference between $C(\pi^+\pi^+)$ and $C(\pi^-\pi^-)$
- ◆ Likely due to the third-body Coulomb and isospin effects

Vinh Luong QM '25 Talk

Fitting the correlation function

Bowler-Sinyukov procedure : $C(\vec{q}) = N [(1 - \lambda) + \lambda K_{\text{Coul}}(q_{\text{inv}})(1 + G(\vec{q}))]$
 $G(\vec{q}) = \exp(-q_o^2 R_o^2 - q_s^2 R_s^2 - q_l^2 R_l^2 - 2q_o q_l R_{ol}^2)$

❖ **N : normalization factor, λ : correlation strength factor**

❖ **K_{coul} : two-pion Coulomb correlation function**

❖ **$R_{\text{out}} \propto$ geometrical size and emission duration**

❖ **$R_{\text{side}} \propto$ geometrical size**

M.G. Bowler, PLB 270, 69 (1991)

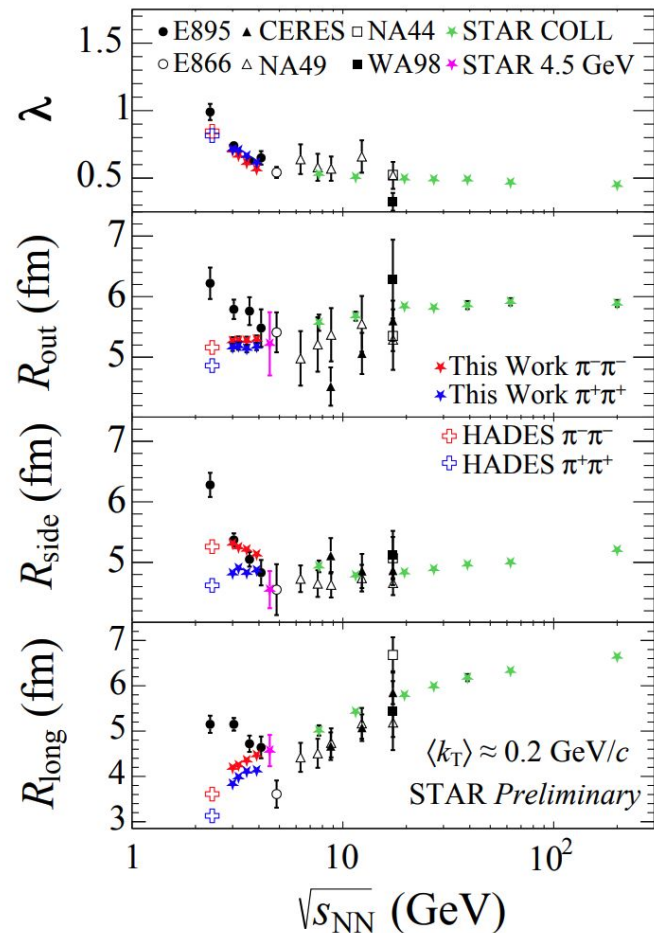
Yu.M. Sinyukov, et. al., PLB 432, 248 (1998)

❖ **$R_{\text{long}} \propto$ source lifetime**

❖ **$R_{\text{out-long}}^2 \propto$ tilt of the correlation functions in the $(q_{\text{out}}, q_{\text{long}})$ plane**

Collision energy dependence

- ❖ Femtoscopic parameters are extracted over a wide range of collision energies
- ❖ The collision energy dependence of femtoscopic radii favour the trend formed by results from HADES and STAR at higher energies.
- ❖ A slight decrease of R_{side} and increase of R_{long} with increasing collision energy are observed as the emitting source evolves from oblate to prolate.



Critical Point searches

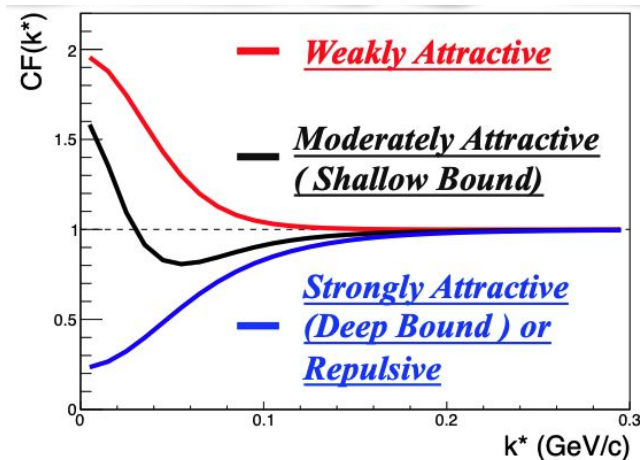
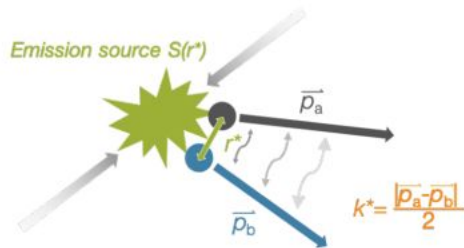
Femtoscscopy

Exotic Nuclei

Exotic Nuclei

Observation of bound states can be experimentally verified through femtoscopic correlation functions.

Hyperon-Nucleon (Y-N) and Hyperon-Hyperon (Y-Y) interactions provide important information to constrain the Equation-of-State and help to understand the inner structure of compact stars



$$C(k^*) = \int S(r^*) \underbrace{\left\| \Psi(k^*, r^*) \right\|^2}_{\text{Model}} d^3 r^* = \underbrace{\frac{A(k^*)}{B(k^*)}}_{\text{Measurement}}$$

Lednický-Lyuboshitz Model

$$CF(k^*) = \int d^3r^* S(r^*) |\psi(r^*, k^*)|^2 = \frac{N_{same}(k^*)}{N_{mixed}(k^*)}$$

➤ Wave function:

$$\square \quad \psi(r^*, k^*) = e^{-ik^*r^*} + f(k^*) \frac{e^{-ik^*r^*}}{r^*}$$

➤ Scattering amplitude:

$$\square \quad f(k^*) = \left[\frac{1}{f_0} + \frac{1}{2} d_0 k^{*2} - ik^* \right]^{-1} \text{ (No Coulomb)}$$

$$\square \quad f(k^*) = \left[\frac{1}{f_0} + \frac{1}{2} d_0 k^{*2} - \frac{2}{a_c} h(\eta) - ik^* A_c(\eta) \right]^{-1} \text{ (Include Coulomb)}$$

$$a_c: \text{Bohr radius} \quad \eta = (k^* a_c)^{-1}$$

$$A_c, h: \text{Coulomb interaction factor}$$

➤ Physics quantity:

$$\square \quad f_0: \text{Scattering Length}$$

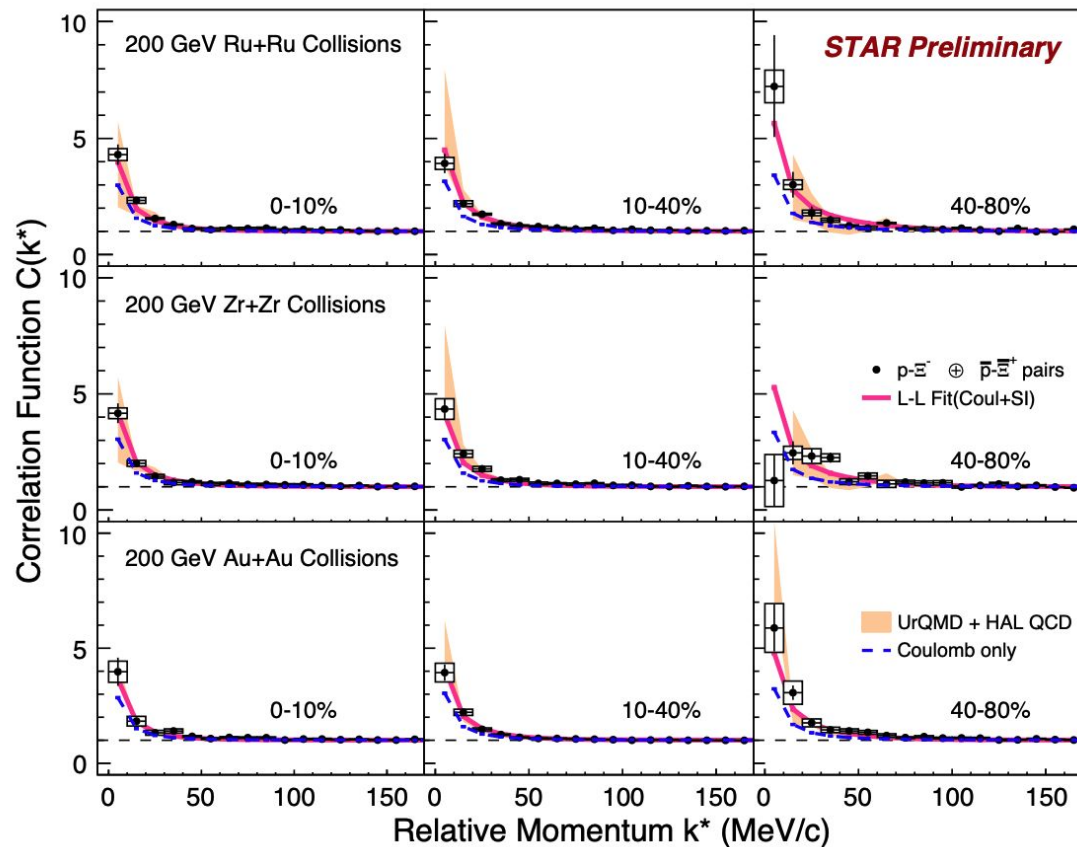
$$\square \quad d_0: \text{Effective Range}$$

$$\square \quad R_G: \text{Spherical Gaussian Source Size}$$

***Simultaneously fit with L-L function for different centralities in each collision system to extract f_0, d_0, R_G by Bayesian method**

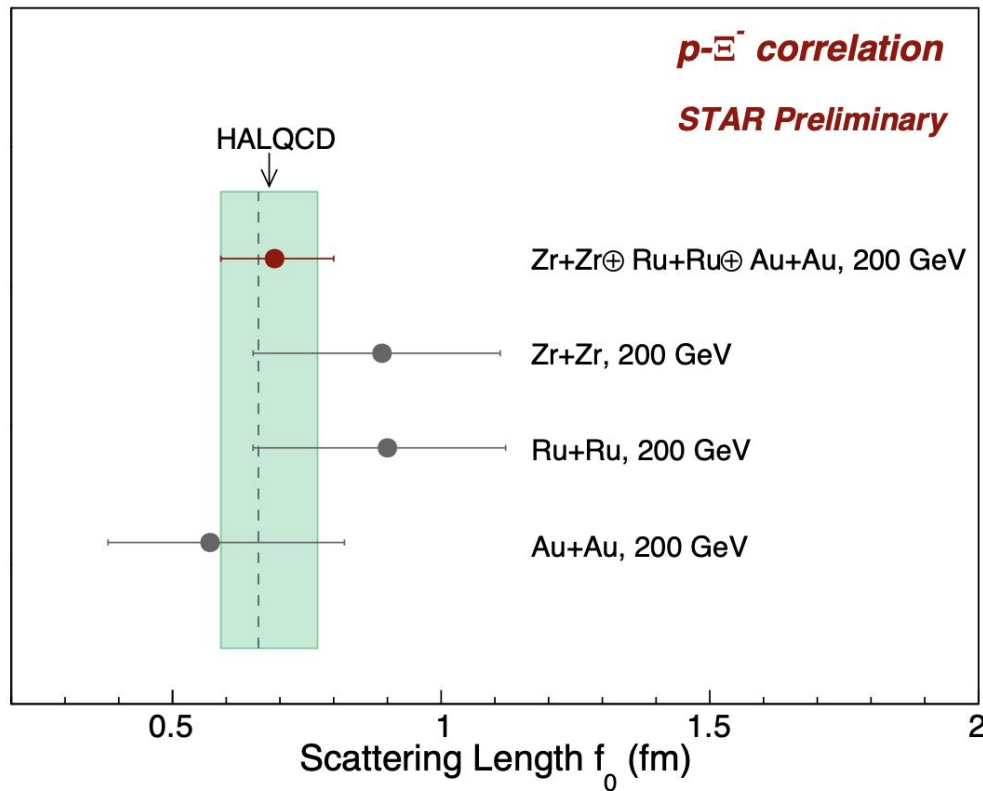
R. Lednický and V. L. Lyuboshitz,
Sov. J. Nucl. Phys. 35, 770 (1982)

Correlation functions: $p - \Xi^- \oplus \bar{p} - \Xi^+$



- ◆ Correlation functions in 200 GeV Au+Au, Ru+Ru and Zr+Zr
- ◆ Enhancement seen at low k^*
- ◆ Models able to describe measurements well
- ◆ Dibaryon $\leftrightarrow p \oplus \Xi^-$??

LL fit to CF

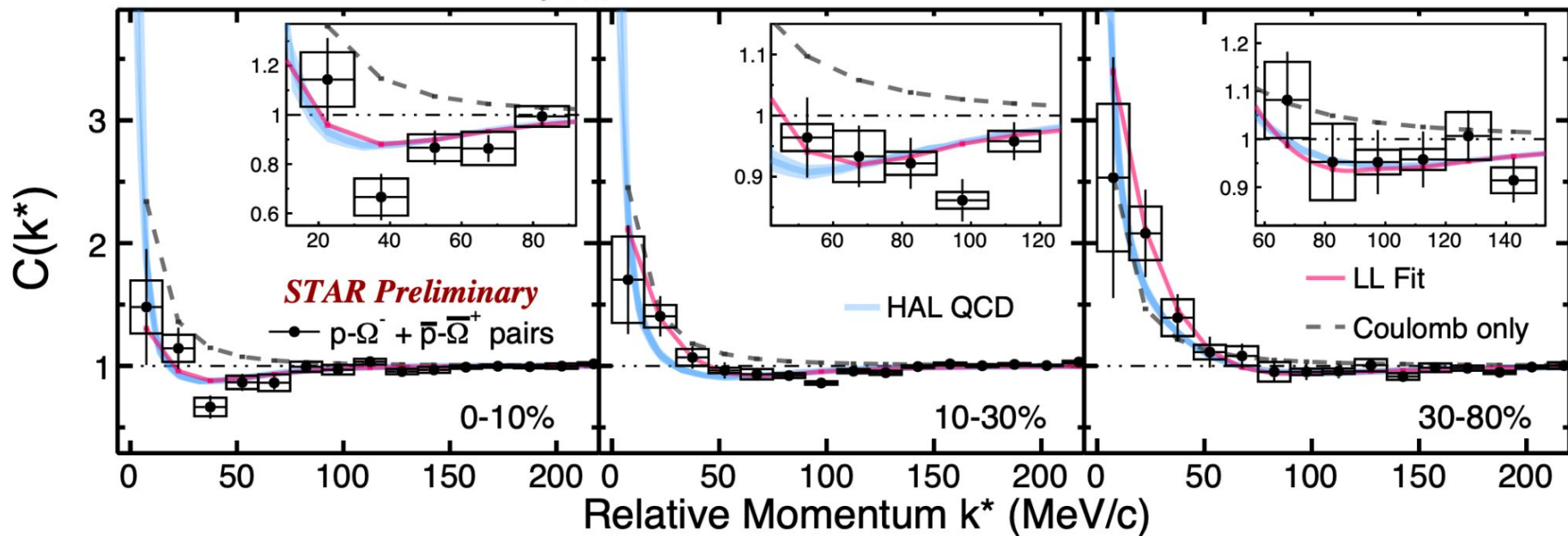


- ❖ Simultaneous fit for different centralities in each collision system to extract f_0 by Bayesian method
- ❖ First experimental constraints of strong interactions parameters in heavy-ion collisions
- ❖ Extracted $f_0 = 0.7^{+0.1}_{-0.1}$ fm
- ❖ Weakly attractive interaction
- ❖ Consistent with HAL QCD prediction

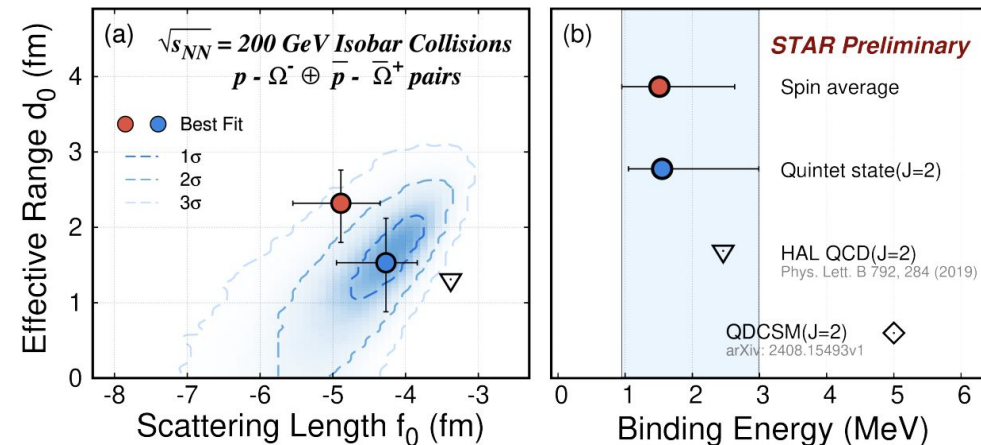
Correlation functions: $p - \Omega^- \oplus \bar{p} - \bar{\Omega}^+$



$\sqrt{s_{NN}} = 200 \text{ GeV Isobar Collisions}$



LL fit to CF



◆ Extracted negative f_0

➤ **First experimental evidence of Strange Dibaryon**

◆ Calculated binding energy consistent with HAL QCD prediction

$$\text{Reduced mass: } m_{p\Omega} = \frac{m_p m_\Omega}{m_p + m_\Omega}$$

$$BE_{p\Omega} = \frac{1}{2m_{p\Omega}d_0^2} \left(1 - \sqrt{1 + \frac{2d_0}{f_0}} \right)^2$$

	Spin ave.	Quintet	HAL QCD
f_0 (fm)	$-4.9^{+0.5}_{-0.7}$	$-4.3^{+0.4}_{-0.7}$	-3.4
d_0 (fm)	$2.3^{+0.4}_{-0.5}$	$1.5^{+0.5}_{-0.7}$	1.3
BE (MeV)	$1.5^{+1.1}_{-0.6}$	$1.6^{+1.4}_{-0.5}$	2.3

Kenji Morita, et al., Phys. Rev. C 101, 015201 (2020)

Kehao Zhang QM '25 Talk

1. **Proton cumulants:**
 - a. Central C_4/C_2 shows a maximum deviation seen at 19.6 GeV for significance of deviation $\sim 2 - 5\sigma$
 - b. Significant deviations observed at other orders.
2. **2-particle p_T correlator:**
 - a. Centrality dependence deviate systematically from expected power-law scaling behavior.
 - b. Displays significant non-monotonic behavior as a function of collision energy in the 0–5% centrality bin.
3. **Baryon-Strangeness correlations:**
 - a. In central collisions, C_{BS} values are consistent with partonic calculations at 39 and 62.4 GeV, while agrees well with hadronic simulations at 7.7 and 11.5 GeV. Intermediate energies such as 14.6, 19.6 and 27 GeV cannot be reproduced by any calculations.
4. **Extraction of emitting source using femtoscopy:**
 - a. Dynamic properties of the source: emission time, source tilt angle, freeze-out eccentricity, space-time emission asymmetry, are determined
5. **Extraction of final state interaction using femtoscopy:**
 - a. Powerful tool to measure of parameters of strong interactions, first evidence of di-baryon states measured.



Thank
You

***Not all STAR results could be covered in this talk
Stay tuned for more STAR BES-II and FXT results**

1. Temperature Fluctuations in Multiparticle Production - Phys. Rev. Lett. 75, 1044
2. Incident energy dependence of pt correlations at relativistic energies - Phys.Rev.C72:044902,2005
3. Event-by-event fluctuations in mean p_T and mean e_T in $s(NN)^{1/2} = 130$ -GeV Au+Au collisions - Phys.Rev.C 66 (2002) 024901
4. Collision-energy dependence of p_T correlations in Au + Au collisions at energies available at the BNL Relativistic Heavy Ion Collider - Phys.Rev.C 99 (2019) 4, 044918
5. Event-by-event mean p_T fluctuations in pp and Pb-Pb collisions at the LHC - Eur. Phys. J. C 74 (2014) 3077
6. Specific Heat of Matter Formed in Relativistic Nuclear Collisions - Phys.Rev.C 94 (2016) 4, 044901
7. Baryon Stopping and Associated Production of Mesons in Au+Au Collisions at $s(NN)^{1/2}=3.0$ GeV at STAR - Acta Phys. Pol. B Proc. Suppl. 16, 1-A49 (2023)
8. Traces of Thermalization from p_T Fluctuations in Nuclear Collisions - S. Gavin, Phys. Rev. Lett. 92, 162301 (2004)